

Electronic supplementary information for

Fluorinated alloy-type interfacial layer enabled by metal fluoride nanoparticles modification for stabilizing Li metal anode

Feng Li,^a Yi-Hong Tan,^b Yi-Chen Yin,^b Tian-Wen Zhang,^a Lei-Lei Lu,^b Yong-Hui Song,^a Te Tian,^b Bao Shen,^b Zheng-Xin Zhu,^b and Hong-Bin Yao^{*a,b}

- a. Division of Nanomaterials & Chemistry, Hefei National Laboratory for Physical Sciences at the Microscale, University of Science and Technology of China*
- b. Department of Applied Chemistry, CAS Center for Excellence in Nanoscience, Hefei Science Center of CAS, University of Science and Technology of China, 96 Jinzhai Road, Hefei, Anhui 230026, China*

**Email: yhb@ustc.edu.cn*

EXPERIMENTAL SECTION

Chemicals: Diethylene glycol (DEG, >99%, Aladdin), Ammonium fluoride (NH_4F , >99.99%, Aladdin), Zinc nitrate hexahydrate ($\text{Zn}(\text{NO}_3)_2 \cdot 6\text{H}_2\text{O}$, >99.0%, Sinopharm Group Co., Ltd), Ethanol ($\text{C}_2\text{H}_5\text{OH}$, >99.7%, Sinopharm Group Co., Ltd), Calcium nitrate tetrahydrate ($\text{Ca}(\text{NO}_3)_2 \cdot 4\text{H}_2\text{O}$, >99.0%, Sinopharm Group Co., Ltd), Magnesium nitrate hexahydrate ($\text{Mg}(\text{NO}_3)_2 \cdot 6\text{H}_2\text{O}$, >99.0%, Sinopharm Group Co., Ltd), Aluminum nitrate nonahydrate ($\text{Al}(\text{NO}_3)_3 \cdot 9\text{H}_2\text{O}$, >99.0%, Sinopharm Group Co., Ltd), 1,3-dioxolane (DOL, 99.8%, Aladdin), 1, 2-dimethoxyethane (DME, 99.5%, Aladdin), Tetrahydrofuran (THF, 99.8%, Energy chemical), Super-P acetylene black (Alfa Aesar), Polyvinylidene fluoride (PVDF, Sigma-Aldrich), N-Methyl-2-pyrrolidone (NMP, Sigma-Aldrich). The above chemicals were purchased and used without further purification.

Synthesis of MF_x NPs (M=Zn, Ca, Mg, Al): All chemical reagents were used as received without further purification. The typical recipe for the polyol-mediated synthesis of monocrystalline CaF_2 was applied to prepare MF_x NPs. First, 50 mL DEG was put into a three-neck flask (volume 100 mL) under the atmosphere of nitrogen under vigorous magnetic stirring. 16 mmol of NH_4F was added into the above solution with heating to 100 °C to dissolve the NH_4F . Besides, 8 mmol $\text{Zn}(\text{NO}_3)_2 \cdot 6\text{H}_2\text{O}$ was dissolved into another 10 mL DEG to become a clear and transparent solution heated at 80 °C. Then, the later solution was added into the former one by injection under the heating at 80 °C. After 5 min stirring, the mixture suspension solution was rapidly heated to 120 °C within 5 min and cooled to room temperature after maintaining another 5 min. The solid nanoparticles were collected by several times of centrifugation (15 min, 12 000 rpm) washed by ethanol to remove excess DEG and remaining salts. The collected solid nanoparticles can be used after drying in a vacuum oven at 100 °C. The preparation process of other metal fluoride nanoparticles (CaF_2 , MgF_2 , AlF_3) is similar to the above synthetic process only replacing $\text{Zn}(\text{NO}_3)_2 \cdot 6\text{H}_2\text{O}$ by the corresponding stoichiometric $\text{Ca}(\text{NO}_3)_2 \cdot 4\text{H}_2\text{O}$, $\text{Mg}(\text{NO}_3)_2 \cdot 6\text{H}_2\text{O}$ and $\text{Al}(\text{NO}_3)_3 \cdot 9\text{H}_2\text{O}$, respectively.

Preparation of MF_x NPs dispersed in DOL/DME (1:1, v/v): All processes are carried out in an argon-

filled glove box ($\text{H}_2\text{O} < 0.5 \text{ ppm}$; $\text{O}_2 < 2.0 \text{ ppm}$). Desired amount of dried MF_x NPs was dispersed into the 15 mL of mixed transparent solution, which consists of DOL and DME with volume ratio of 1 :1, enabling the concentration of MF_x NPs is 90 mM. Then the suspension was stirred vigorously for several hours before use.

Ex-situ chemical modification of Li metal foil by MF_x NPs suspension: All processes are carried out in an argon-filled glove box ($\text{H}_2\text{O} < 0.5 \text{ ppm}$; $\text{O}_2 < 2.0 \text{ ppm}$). The oxide layer on the surface of Li metal foil was removed carefully with a soft nylon brush and THF. Then the fresh Li metal foil was put into the as-prepared MF_x NPs suspension, in which MF_x NPs are uniformly dispersed. After treated by heating to $45 \text{ }^\circ\text{C}$ for 8 h, the surface color of protected Li metal foil is different from the pristine Li metal foil as shown in Fig. S3 (ESI[†]). After washing the protected Li metal foil with DOL for several times the excess DOL on the surface of as-obtained Li metal foil were removed in the vacuum chamber before the characterization and assembling batteries.

Characterizations: X-ray diffraction (XRD) patterns of MF_x NPs were collected on a Philips X'Pert PRO SUPER X-ray diffractometer equipped with graphite monochromatized $\text{Cu K}\alpha$ radiation. The nanostructure and morphology of MF_x NPs was revealed by transmission electron microscope (TEM, Hitachi H-7650). Scanning electron microscopy (SEM, JEOL-6700F) was applied to characterize the morphologies evolution and elemental mapping of the protected Li by MF_x NPs before and after cycling, respectively. X-ray photoelectron spectrometer (XPS, ESCALAB 250, Thermo-VG Scientific) was employed to analyze the chemical compositions of the protected Li metal anode by MF_x NPs before and after cycling, respectively.

Electrochemical Measurements: 2032-type coin cells were assembled in an argon-filled glove box with water and oxygen contents $< 0.5 \text{ ppm}$ and 2.0 ppm , respectively. For the cathode of Li-metal-based battery, $\text{LiNi}_{0.8}\text{Co}_{0.15}\text{Al}_{0.05}\text{O}_2$ (NCA), super-P acetylene black and PVDF was mixed with a weight ratio of 80:10:10 in the NMP solvent to form a uniform slurry after grinding for 1 h. Then the obtained slurry was coated onto the surface of Al-carbon foil (MTI) by doctor blade and dried at $80 \text{ }^\circ\text{C}$ in vacuum oven. A polyethylene separator from Celgard was used as a separator and 1.0 M LiPF_6 in EC/DEC/DMC (1:1:1,

v/v/v) was employed as the electrolyte. The plating/stripping stability of symmetric cells and cycle performances of full Li-metal-based batteries were evaluated on LAND multichannel electrochemical testing system. Bio-Logic VMP3 electrochemical working station was used to record the electrochemical impedance spectroscopy (EIS) with frequency set between 1M Hz and 1 Hz.

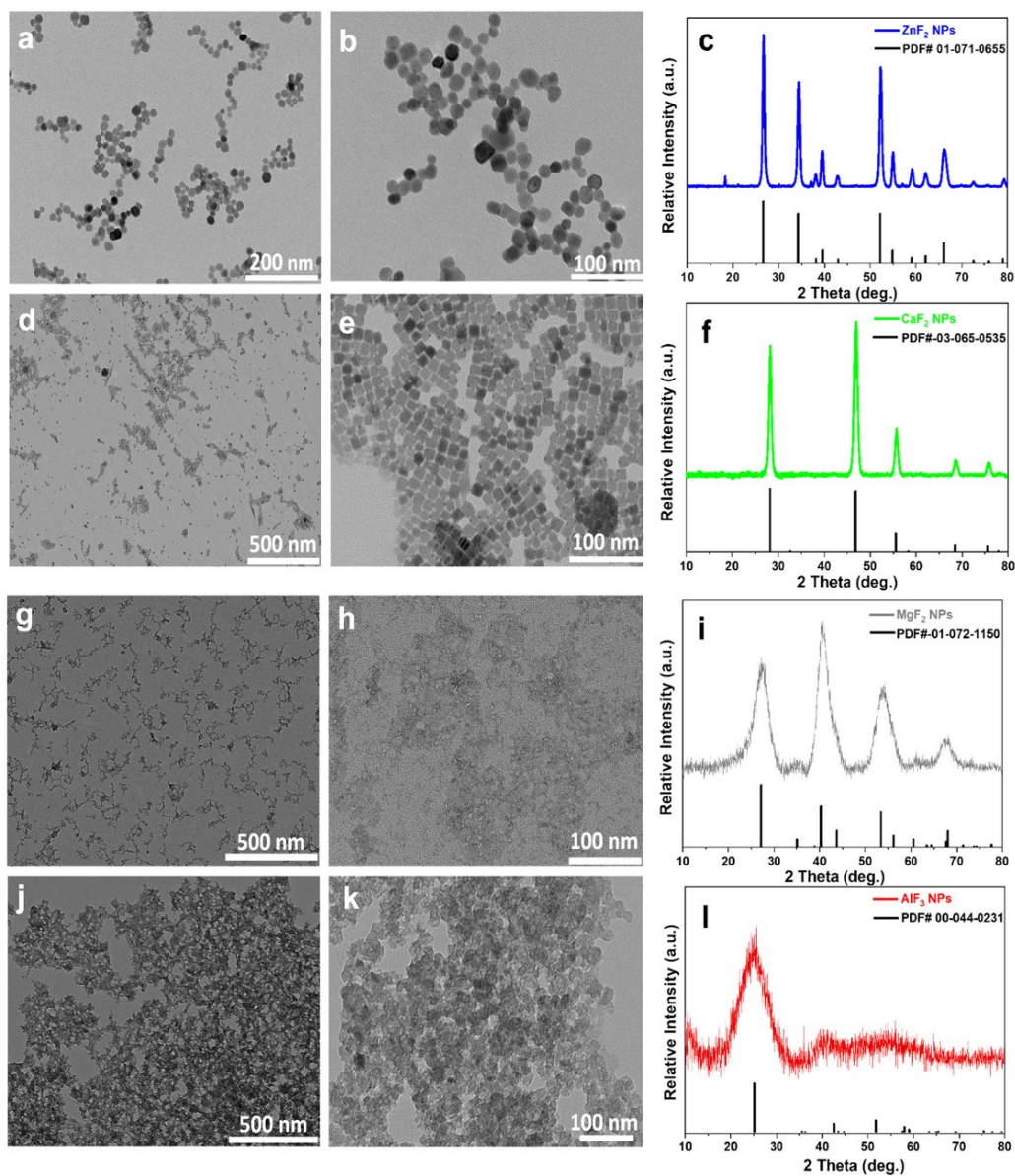


Figure S1. (a, b) TEM images and (c) XRD pattern of ZnF₂ NPs. (d, e) TEM images and (f) XRD pattern of CaF₂ NPs. (g, h) TEM images and (i) XRD pattern of MgF₂ NPs. (j, k) TEM images and (l) XRD pattern of AlF₃ NPs.

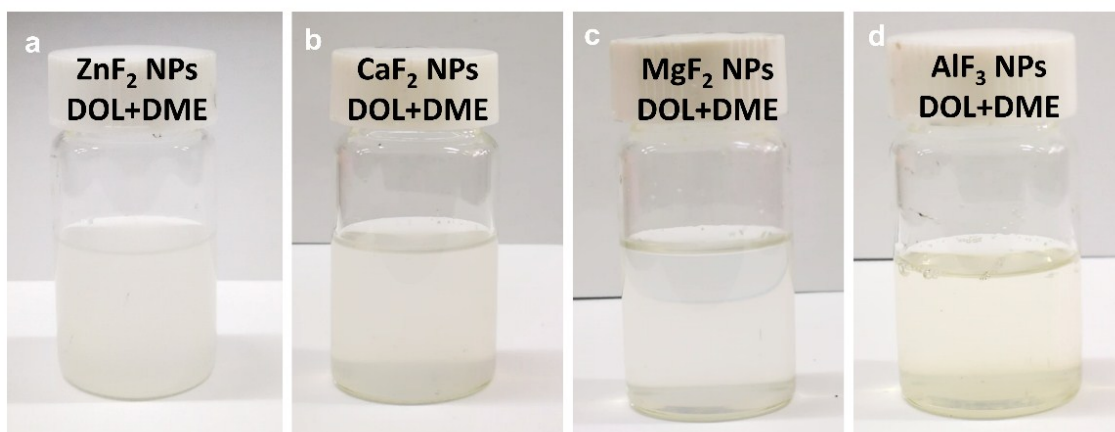


Figure S2. (a-d) Optical photographs of a DOL/DME co-solvent dispersed ZnF₂, CaF₂, MgF₂ and AlF₃ NPs, respectively.

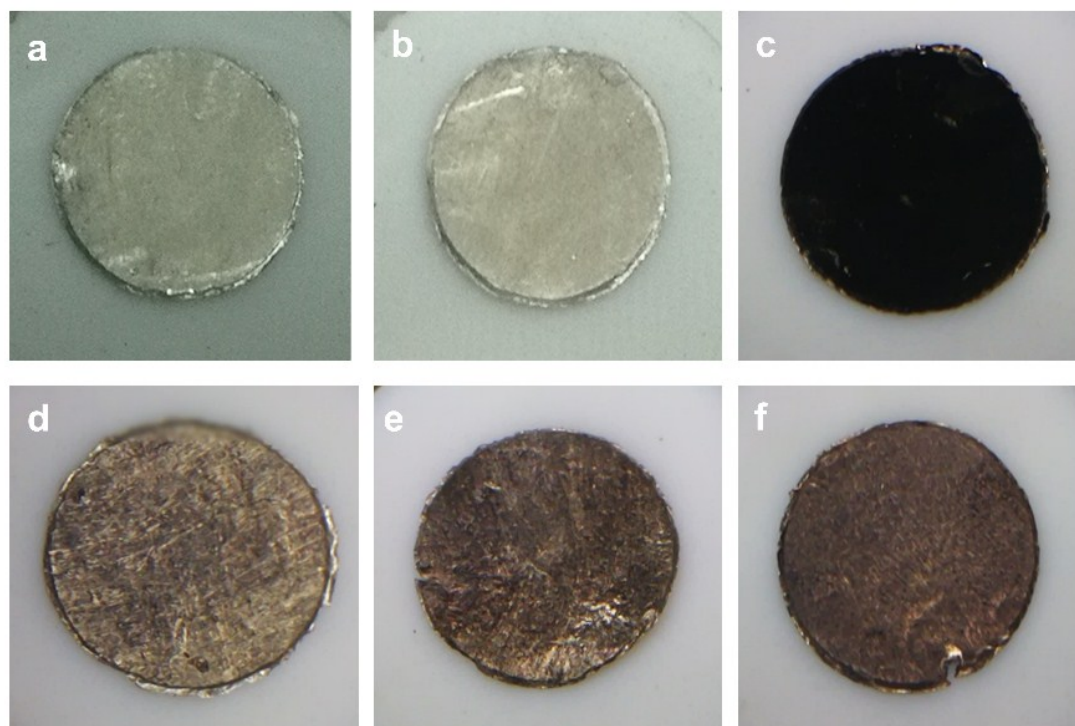


Figure S3. Optical photographs of (a) a pristine Li foil. (b) the Li foil treated by pure co-solvent DOL/DME (1:1, v/v). (c-f) Protected Li treated by co-solvent dispersed ZnF₂, CaF₂, MgF₂ and AlF₃ NPs, respectively.

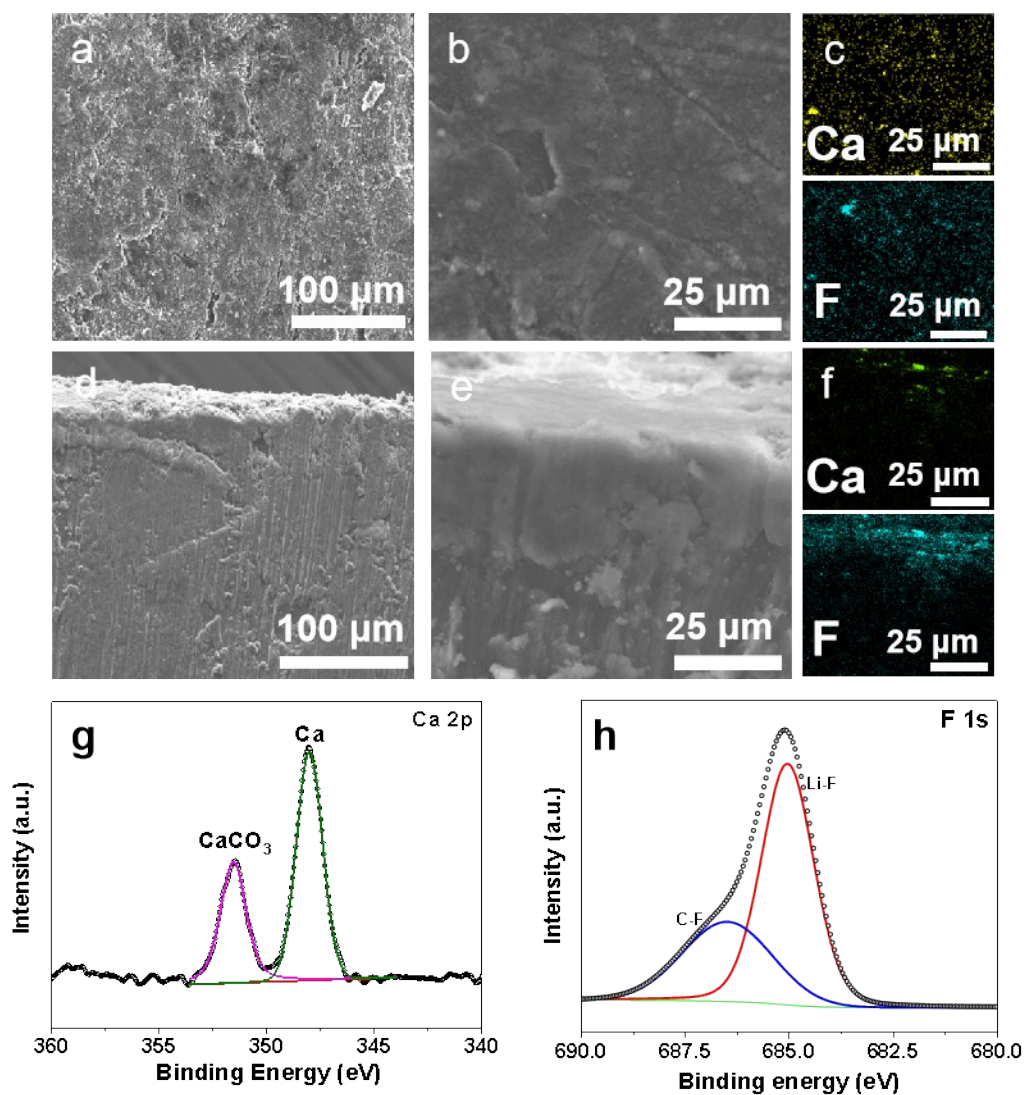


Figure S4. (a, b) The top-view SEM images, (c) corresponding EDX mapping analysis, (c, d) side-view SEM images and (e) corresponding EDX mapping analysis of CaF₂ NPs – treated Li metal anode. (g-h) The Ca 2p, F 1s XPS analysis of corresponding ASEI layer.

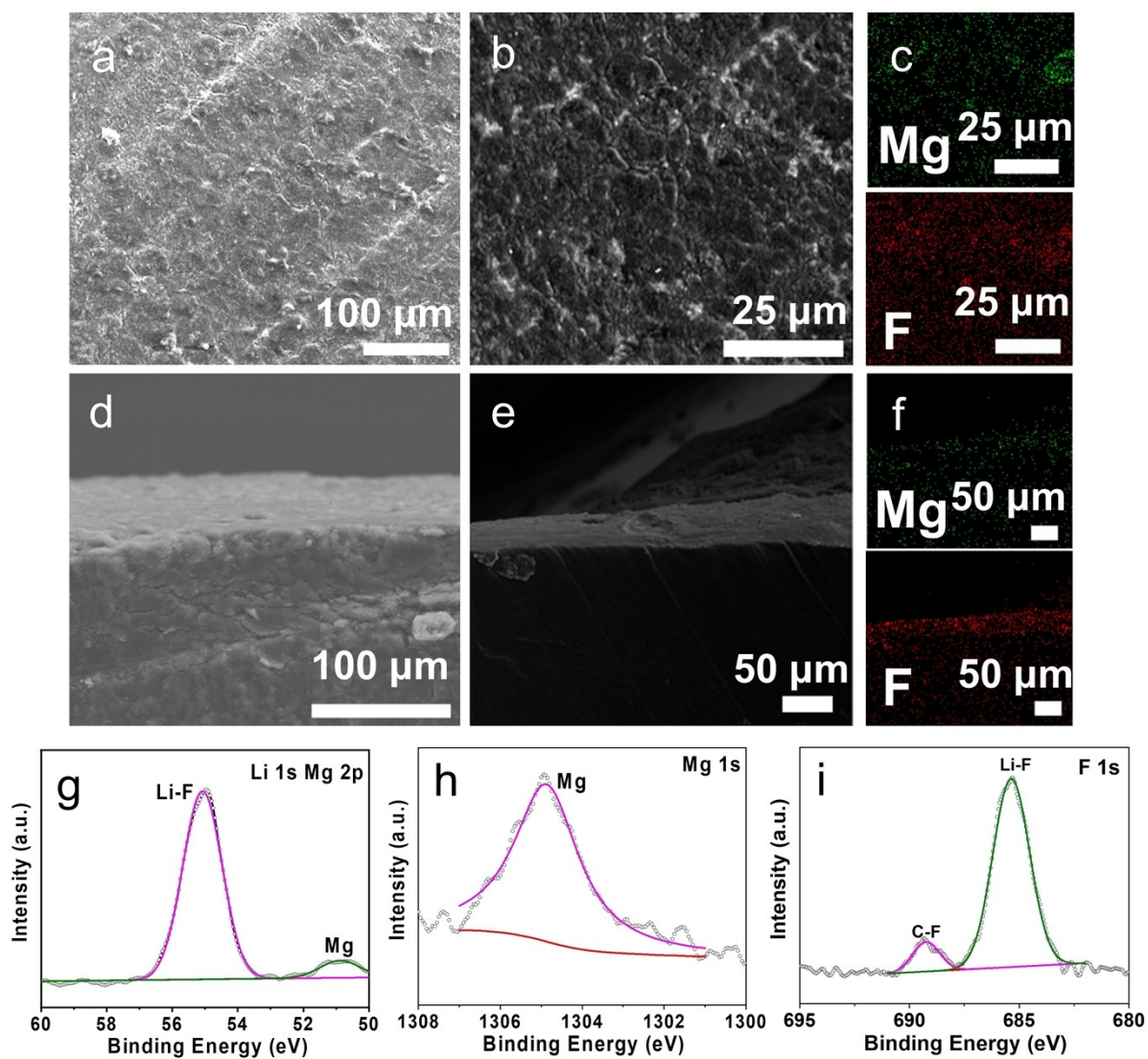


Figure S5. (a, b) The top-view SEM images, (c) corresponding EDX mapping analysis, (c, d) side-view SEM images and (e) corresponding EDX mapping analysis of MgF₂ NPs – treated Li metal anode. (g-h) The Mg 2p, Mg 1s and F 1s XPS analysis of corresponding ASEI layer.

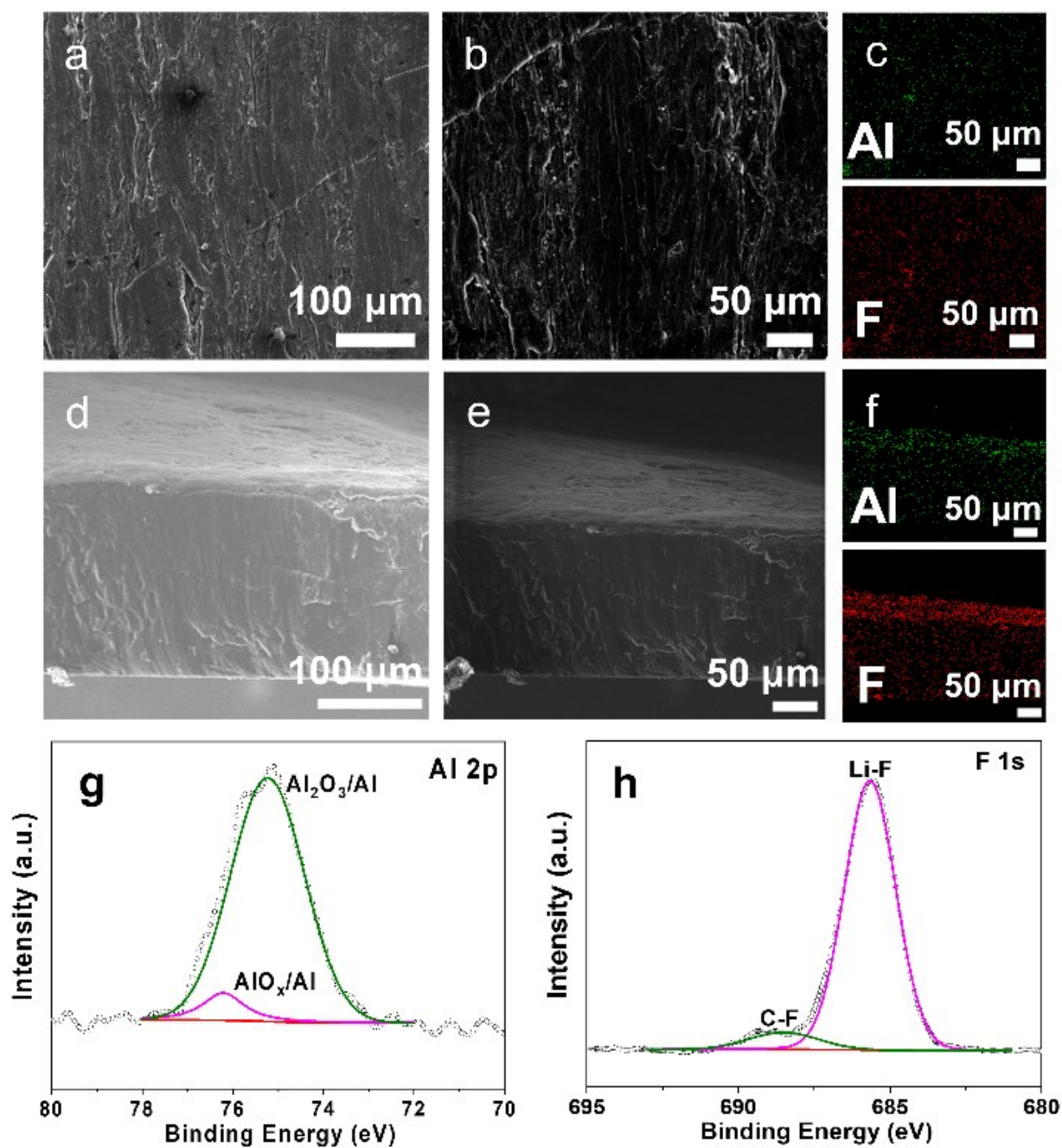


Figure S6. (a, b) The top-view SEM images, (c) corresponding EDX mapping analysis, (c, d) side-view SEM images and (e) corresponding EDX mapping analysis of AlF₃ NPs – treated Li metal anode. (g-h) The Al 2p, F 1s XPS analysis of corresponding ASEI layer.

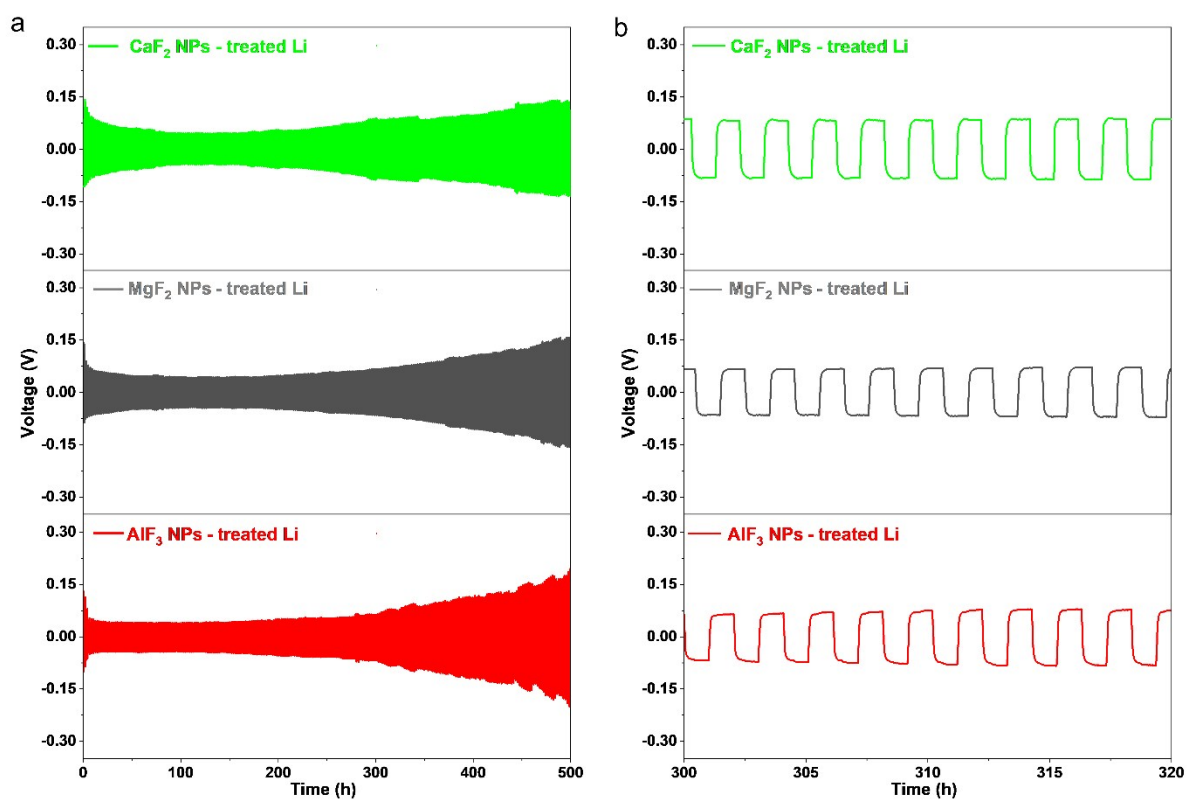


Figure S7. (a) The evolution of voltage profiles of symmetric cells based on MF_x NPs – treated Li metal anode (M=Ca, Mg, Al). (b) The corresponding voltage profiles of (a) in an enlarged view of 300-320 h.

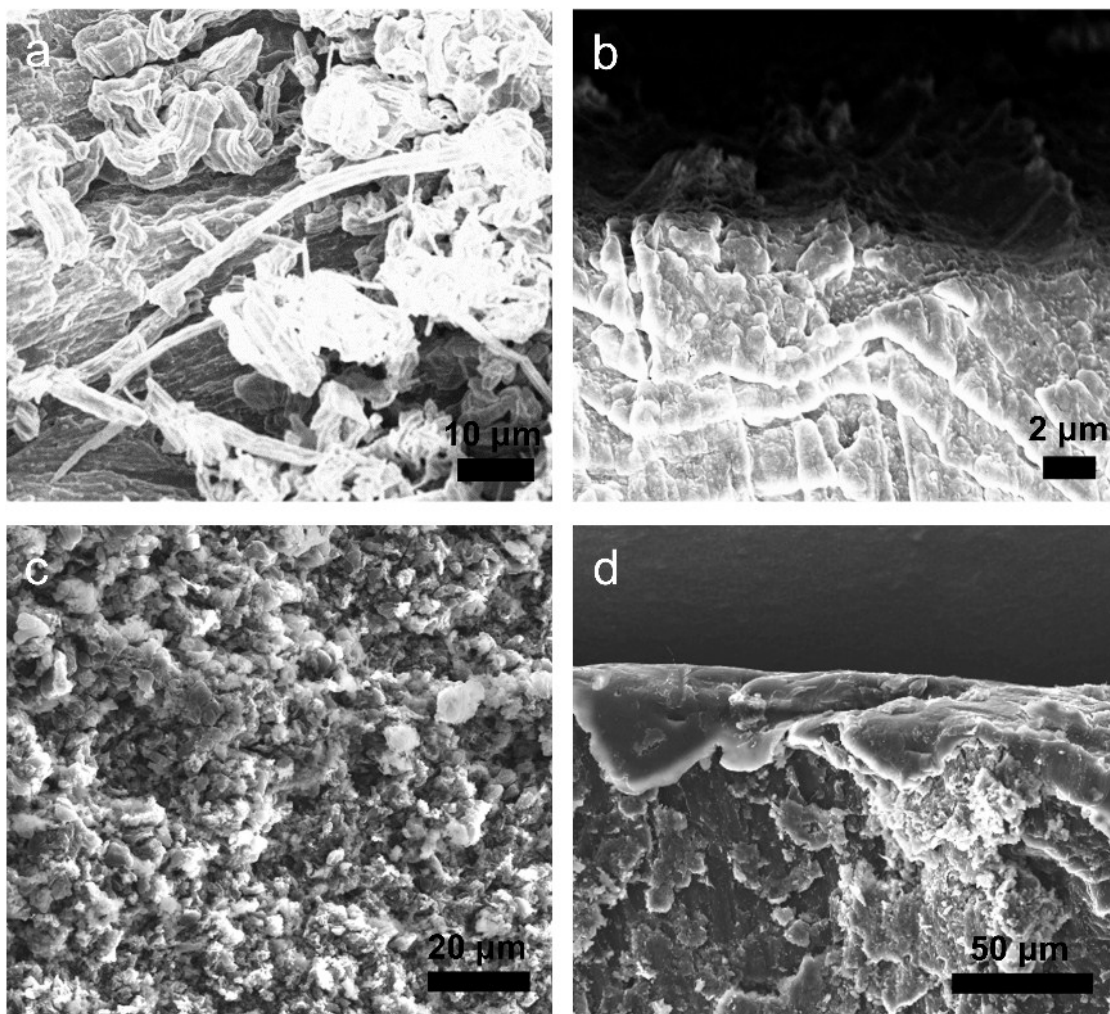


Figure S8. (a)-(c) The top-view and (b)-(d) side-view SEM images of pristine Li metal anode after 2 h and 160 h cycling, respectively.

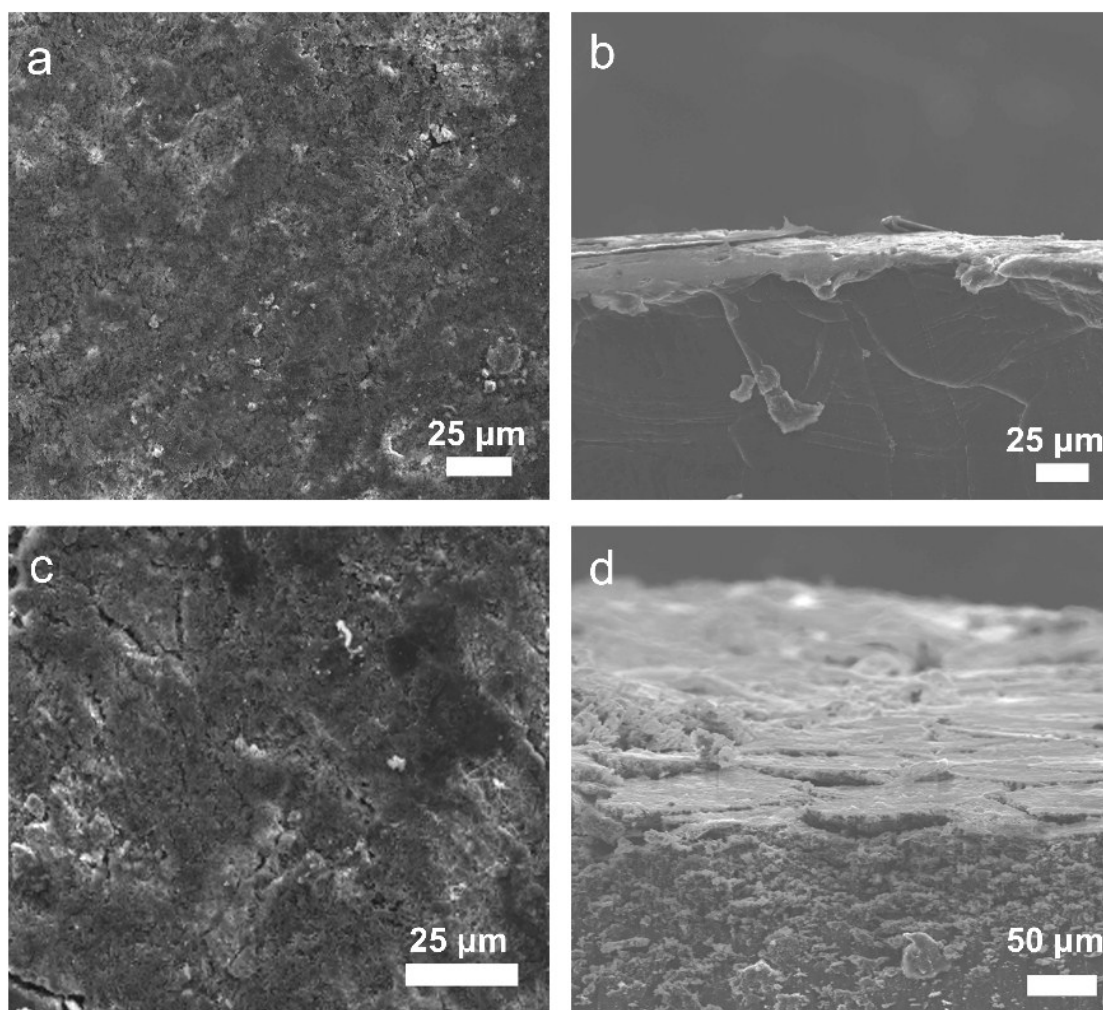


Figure S9. (a)-(c) The top-view and (b)-(d) side-view SEM images of ZnF_2 NPs – treated Li after 2 h and 160 h cycling, respectively.

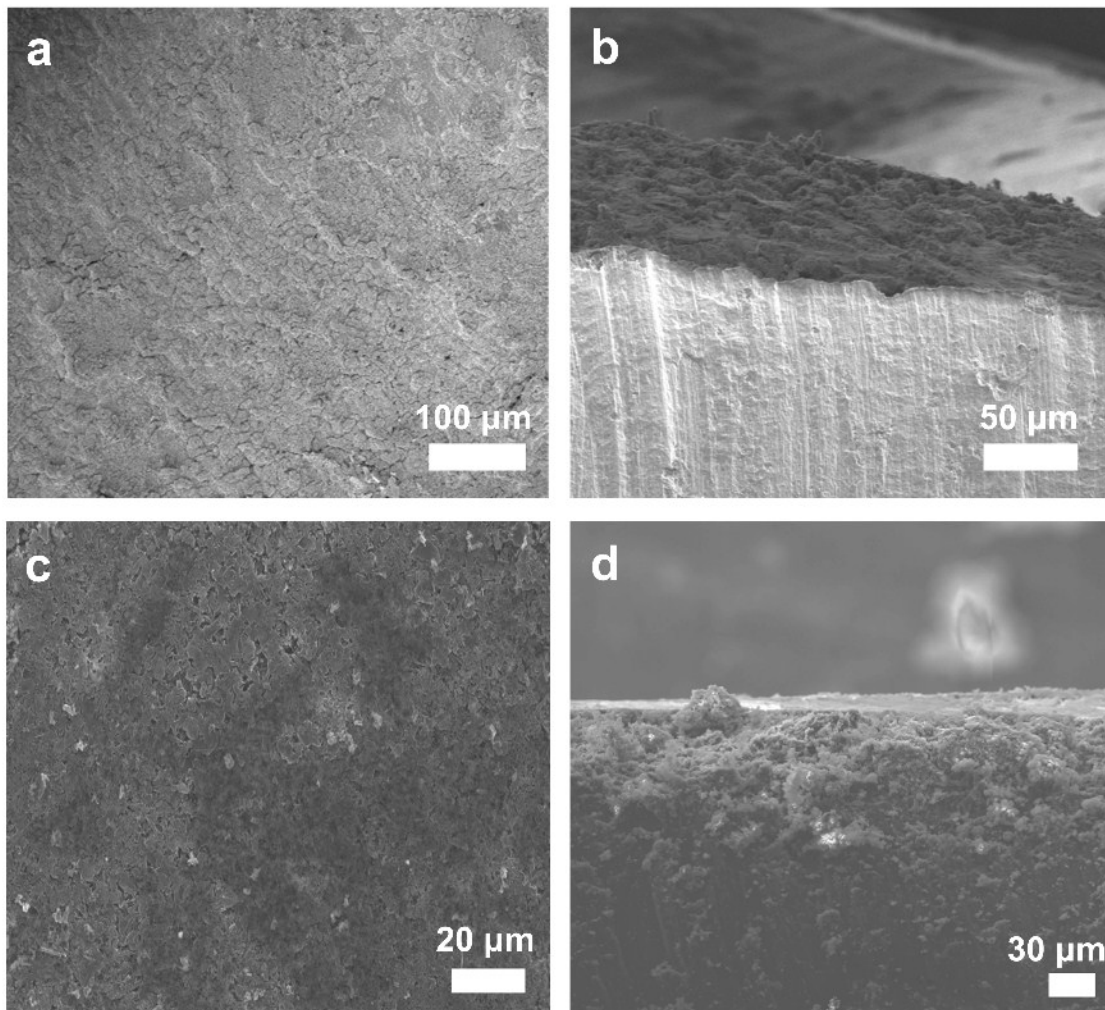


Figure S10. (a)-(c) The top-view and (b)-(d) side-view SEM images of AlF_3 NPs – treated Li metal anode after 2 h and 160 h cycling, respectively.

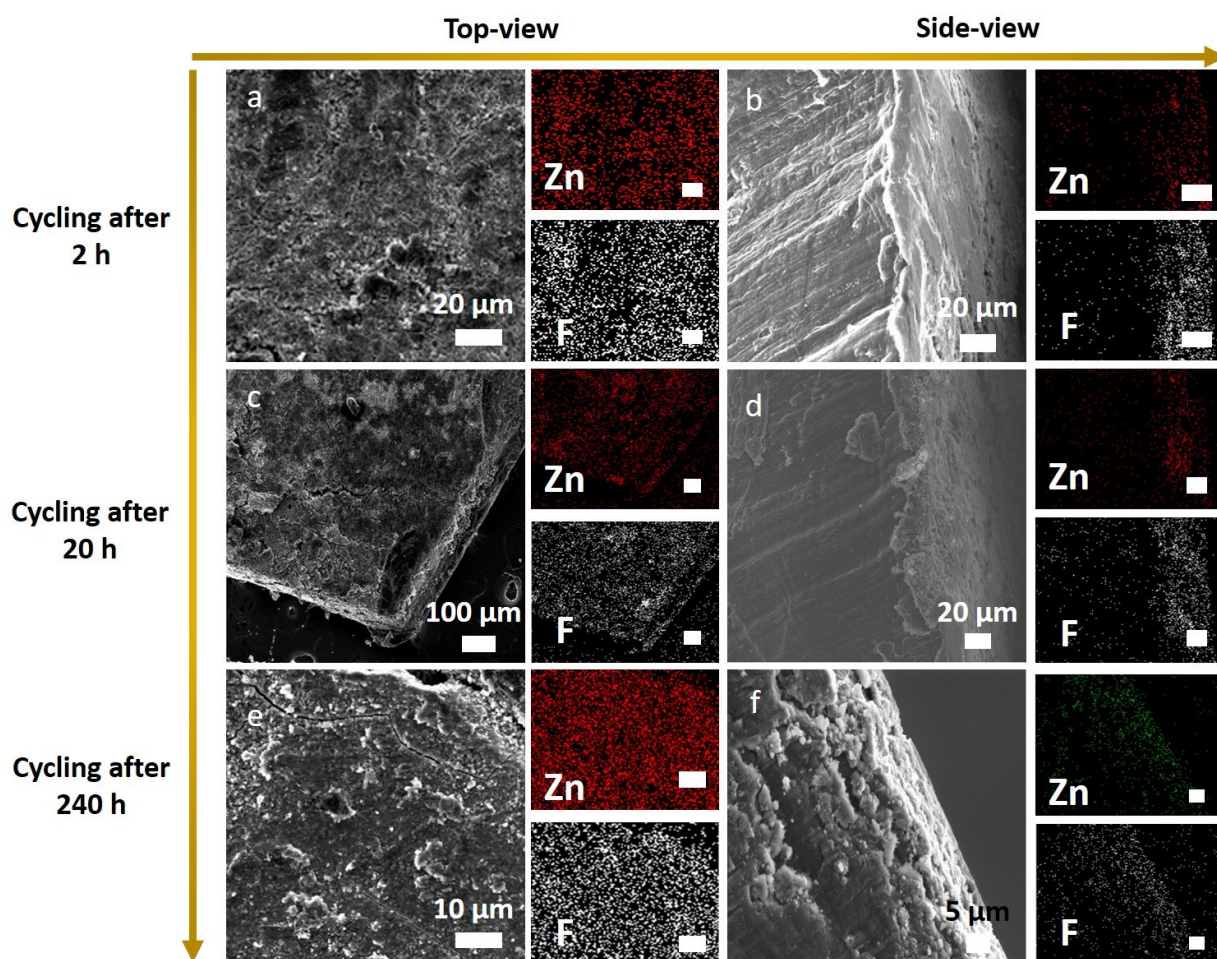


Figure S11. SEM images and corresponding EDX of ZnF₂ NPs-treated Li metal anode after (a-b) 2 h, (c-d) 20 h, and (e-f) 240 h cycling at 1 mA cm⁻²/1 mA h cm⁻², respectively. The scale bars of EDX mapping are the same as that in the corresponding SEM images.

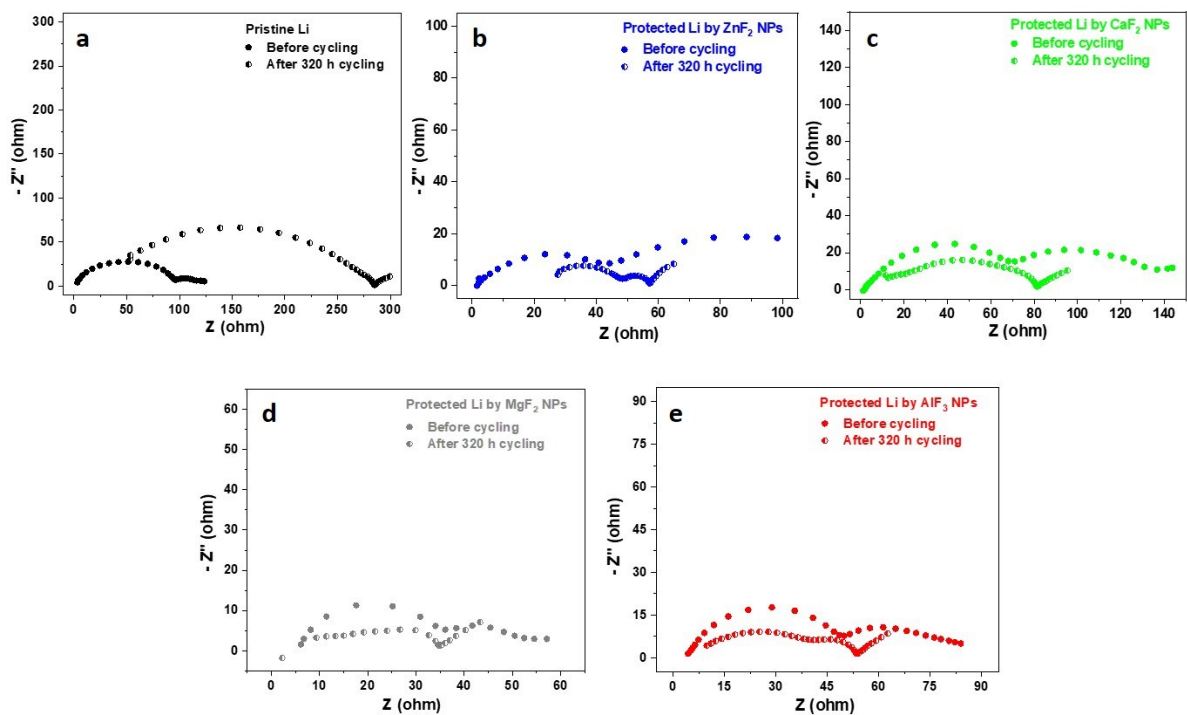


Figure S12. Electrochemical impedance spectra for the symmetric cells based on (a) pristine Li, (b) ZnF_2 NPs – treated Li metal anode, (c) CaF_2 NPs – treated Li metal anode, (d) MgF_2 NPs – treated Li metal anode and (e) AlF_3 NPs – treated Li metal anode, respectively.

Table S1. The comparison of related studies on stabilizing Li-metal deposition

Optimizing Strategy	Methods	Electrolyte (liquid)	I (mA cm ⁻²)	Cap. (mA h cm ⁻²)	Voltage (mV)	Cycle-Life (hours)	Ref.
LiBOB	Additive	1.0 M LiPF ₆ in EC/EMC/DEC 3:5:2	1.0	1.0	~250	350	1
BTfE&LiDFOB	Additive	1 M LiPF ₆ in EC/EMC (3:7) with 2 wt% VC	1.0	1.0	~250	550	2
			2.0	1.0	~400	170	2
LiF/Li _x In _y	Additive	1.0 M LiPF ₆ in EC/DMC 1:1	1.0	1.0	~200	400	3
Li ₂ TiO ₃ (LT) layer	Sol-Gel	1.3 M LiPF ₆ in EC/DEC (3:7) with 10 wt% FEC	1.0	1.0	~220	350	4
Amorphous Li ₃ PO ₄	Magnetron Sputtering	1 M LiPF ₆ in EC/DEC/DMC 1:1:1	1.0	1.0	~260	300	5
PVDF-HFP LiF	Doctor Blade	1.0 M LiTFSI in DOL/DME 1:1	2.0	1.0	~100	200	6
LiF	Magnetron Sputtering	1 M LiTFSI in PC	1.0	1.0	~100	160	7
Al ₂ O ₃	ALD	1M LiPF ₆ in EC/DMC 1:1	1.0	0.25	~190/600	350/500	8
<i>LiF/Li-Zn Alloy layer</i>	<i>Chemical Modification</i>	<i>1.0 M LiPF₆ in EC/DEC/DMC 1:1:1</i>	<i>1.0</i>	<i>1.0</i>	<i>~90/~200</i>	<i>400/500</i>	<i>Our work</i>
			<i>2.0</i>	<i>2.0</i>	<i>~200</i>	<i>200-250</i>	

The reference in the table as follow.

- [1] ACS Appl. Mater. Interfaces 2019, 11, 20854–20863
- [2] ACS Energy Lett. 2018, 3, 2059–2067
- [3] Angew. Chem. Int. Ed. 2018, 57, 1-5
- [4] Adv. Energy Mater. 2019, 1803722
- [5] Journal of Power Sources 342 (2017) 175e182
- [6] Adv. Funct. Mater. 2018, 28, 1705838
- [7] J. Mater. Chem. A, 2017, 5, 3483–3492
- [8] Chem. Mater. 2015, 27, 6457–6462